

Optimizing WIMP directional detectors

Anne M. Green¹, Ben Morgan²

¹*School of Physics and Astronomy, University of Nottingham, University Park, Nottingham, NG7 2RD, UK.*

²*Department of Physics, University of Warwick, Coventry, CV4 7AL, UK.*

Abstract

We study the dependence of the exposure required to directly detect a WIMP directional recoil signal on the capabilities of a directional detector. Specifically we consider variations in the nuclear recoil energy threshold, the background rate, whether the detector measures the recoil momentum vector in 2 or 3 dimensions and whether or not the sense of the momentum vector can be determined. We find that the property with the biggest effect on the required exposure is the measurement of the momentum vector sense. If the detector cannot determine the recoil sense, the exposure required is increased by an order of magnitude for 3-d read-out and two orders of magnitude for 2-d read-out. For 2-d read-out the required exposure, in particular if the senses can not be measured, can be significantly reduced by analyzing the reduced angles with the, time dependent, projected direction of solar motion subtracted. The background rate effectively places a lower limit on the WIMP cross-section to which the detector is sensitive; it will be very difficult to detect WIMPs with a signal rate more than an order of magnitude below the background rate. Lowering the energy threshold also reduces the required exposure, but only for thresholds above 20 keV.

Key words:

dark matter, directional detection

PACS: 95.35+d,

1 Introduction

Weakly Interacting Massive Particle (WIMP) direct detection experiments aim to directly detect non-baryonic dark matter via the elastic scattering of

¹ anne.green@nottingham.ac.uk

² ben.morgan@warwick.ac.uk

WIMPs on detector nuclei [1], and are presently reaching the sensitivity required to detect the lightest neutralino (which in most supersymmetry models is the lightest supersymmetric particle and an excellent WIMP candidate). Since the expected event rates are very small ($\mathcal{O}(10^{-5} - 1)$ counts $\text{kg}^{-1}\text{day}^{-1}$) distinguishing a putative WIMP signal from backgrounds due to, for instance, neutrons from cosmic-ray induced muons or natural radioactivity, is crucial. The Earth's motion about the Sun provides two potential WIMP smoking guns: i) an annual modulation [2] and ii) a strong direction dependence [3] of the event rate. The dependence of the differential event rate on the atomic mass of the detector (see e.g. Refs. [4–6]) is a third possibility, however this would require good control of systematics for detectors composed of different materials.

The direction dependence of the WIMP scattering rate has several advantages over the annual modulation. Firstly, the amplitude of the annual modulation is typically of order a few per-cent [2,5] while the event rate in the direction of solar motion is roughly an order of magnitude larger than that in the opposite direction [3,5]. Secondly, it is difficult for the directional signal to be mimicked by backgrounds. In most cases (a point source in the lab is a possible exception) a background which is anisotropic in the laboratory frame will be isotropic in the Galactic rest frame as the time dependent conversion between the lab and Galactic co-ordinate frames will wash out any lab specific features. Low pressure gas time projection chambers (TPCs), such as DRIFT (**D**irectional **R**ecoil **I**dentification **F**rom **T**racks) [7,8] and NEWAGE [9], see also Ref. [10], seem to offer the best prospects for a detector capable of measuring the directions of sub-100 keV nuclear recoils.

Early studies found that in principle as few as 30 events would be required to distinguish a WIMP induced signal from isotropic backgrounds [11,12]. In reality the number of events, and more importantly the required exposure, will depend on the detector properties including the energy threshold, background event rate, whether the read-out measures the recoil momentum in 2 or 3 dimensions (and if 2-d in which plane) [13–15] and whether the sense (i.e. the absolute sign $+\vec{p}$ or $-\vec{p}$) of the recoil momentum vector can be measured [13–15]. In this paper we extend our previous work [13,14] and examine the effects of each of these factors on the number of events, and hence the exposure, required. Our aim is to provide guidance for experimentalists wishing to optimize the detection potential of their experiment. The performance of a real detector will of course be more complex than our simulated detector and the cost (both financial and man-hours) of improvements to the detector performance will in reality have to be taken into account when formulating an optimization strategy. None the less we believe that our results will provide useful indications of which aspects of the detector performance have most effect on the ability to detect a WIMP directional signal.

2 Calculating the Nuclear Recoil Spectrum

We use the same method for calculating the directional nuclear recoil spectrum as in Refs. [13,14]. In this section we explain the essential details, for further information see these references.

2.1 Modeling the Milky Way WIMP halo

We consider the simplest possible model of the Milky Way (MW) halo; an isotropic sphere with density distribution $\rho \propto r^{-2}$. The velocity distribution of WIMPs at all positions within the halo is Maxwellian:

$$f_0(\vec{v}) = \frac{1}{(2\pi/3)^{3/2}\sigma_v^3} \exp\left(\frac{3|\vec{v}|^2}{2\sigma_v^2}\right), \quad (1)$$

where σ_v , the velocity dispersion, is related to the asymptotic circular velocity (which we take to be $v_c = 220 \text{ km s}^{-1}$) by $\sigma_v = \sqrt{3/2} v_c$.

This model is quite possibly not a good approximation to the real Milky Way, however in Refs. [13,14] we found that the number of events required to reject isotropy and detect a WIMP signal changed only weakly for observationally and theoretically motivated smooth halo models. It is possible (see e.g. Refs. [16,17]) that the WIMP distribution on the sub-milli-pc scales which are probed by direct detection is composed of streams. In this case the recoil momentum spectrum, and hence the detectability of WIMPs, would depend strongly on the number and directions of streams passing through the solar neighbourhood.

2.2 Modeling the Detector Response

We model a TPC directional detector filled with 0.05 bar CS_2 , a 10cm drift length over which a uniform drift field of 1kVcm^{-1} is applied and a $200 \mu\text{m}$ 3-d pixel read-out and use the SRIM2003 [18] package to generate sulfur recoil ionisation tracks. The drift and diffusion of this ionisation to the read-out plane by the electric field, together with the generation of charge avalanches, is simulated. The detector properties are chosen based on those of the DRIFT-I/II detectors [8], however we expect that any real TPC based directional detector will have qualitatively similar capabilities.

The recoiling nucleus undergoes a large number of scatterings which, together with the small diffuse of the drifted ionisation, limits the accuracy with which

the direction of the primary recoil can be reconstructed. We reconstruct the recoil track directions using a moment analysis of the pixel charge distributions. In 3-d the distribution of the difference between the primary recoil direction and the reconstructed track direction peaks at $\sim 15^\circ$, decreasing weakly with increasing energy, and has a long large angle tail.

At present no simulations of the angular resolution function of a 2-d detector are available. A 2-d read-out projects the recoil track into a plane and the effects of this combined with multiple scattering and diffusion will make the angular resolution a function of both the energy and primary recoil direction. We therefore assume perfect resolution for 2-d read-out and hence provide lower limits on the numbers of events required for the detection of a WIMP signal with a 2-d detector.

2.2.1 Energy threshold

For primary recoil energies below 20 keV the short track length (3-4 pixels) and multiple scattering make it impossible to reconstruct the track direction in our simulated detector. We therefore define the energy threshold as the energy above which recoil directions can be reconstructed. It is important to note that this energy is higher than the energy threshold for simply *detecting* recoils. In addition, it may be lower than the energy above which recoils can be *discriminated* from electron backgrounds. These details will vary from detector to detector.

2.2.2 Measurability of sense

With SRIM2003 generated recoils, we find near uniform distributions of ionisation along the reconstructed recoil tracks and therefore cannot determine the absolute signs of the reconstructed recoil vectors (i.e $+\vec{p}$ or $-\vec{p}$). Never the less, we note that experimental measurements are required to determine whether this absolute sign can in reality be measured or not. For clarity we refer to read-outs where the sense is measurable as vectorial, and those where it is not as axial.

2.3 2-d read-out

A 2-d read-out measures the projection of the recoil momentum vector into a plane P fixed on the Earth. Choosing an arbitrary vector \vec{c} fixed in P allows (projected) recoil directions to be described via the angle ϕ between the projected recoil and \vec{c} . As well as this raw angle, it is useful to measure the

reduced angle ϕ_{red} between the projected recoil direction and the direction of solar motion projected into the plane:

$$\phi_{red} = \phi - \mu_{\odot}(t), \quad (2)$$

where μ_{\odot} is the angle between the (projected) solar motion direction and \vec{c} , and t is the sidereal time at which the recoil occurred.

The degree of anisotropy in the distributions of ϕ and ϕ_{red} , and hence the detectability of a WIMP signal, is dependent on the orientation of P , the direction \vec{m} in which the recoil rate peaks and the Earth's spin axis \vec{s} . The anisotropy will be maximized if i) the distance between \vec{m} and P , over one sidereal day, is minimized (this minimizes smearing caused by projection effects) and ii) the projection \vec{m} into P has minimal motion relative to \vec{c} (minimizing the smearing caused by time-averaging) [14,15]. These requirements are met, for any \vec{m} , if the normal to P is at 90° to the spin axis of the Earth (we refer to this plane as the meridian plane in Ref. [14]). We focus on this plane for all analyses, but comment on the qualitative effect of changing the orientation.

2.4 Background

Zero background is the goal of the next generation of experiments made from low activity materials with efficient gamma rejection and shielding, located deep underground [19]. We investigate the effect of non-zero isotropic background by varying the ratio of the background and signal event rates and also, independently, the background rate.

2.5 Summary

We calculate the directional recoil rate in the rest frame of the detector via Monte Carlo simulation of the spin-independent elastic scattering of ^{32}S nuclei by WIMPs generated from Eq. 1 with, for illustrative purposes, a mass of $m_{\chi} = 100 \text{ GeV}$. As appropriate, we include the detector angular resolution and energy threshold as discussed above. For 3-d read-out we work in coordinates of Galactic longitude l and latitude b . The flux distribution for sulfur recoils is plotted in Fig. 1 for a WIMP-nucleon elastic scattering cross-section $\sigma = 10^{-6} \text{ pb}$ and local density $\rho_0 = 0.3 \text{ GeV cm}^{-3}$.

For 2-d read-out, the distribution of the ϕ angles is generated from the 3-d recoil distribution in the Galactic coordinate system by Monte Carlo simula-

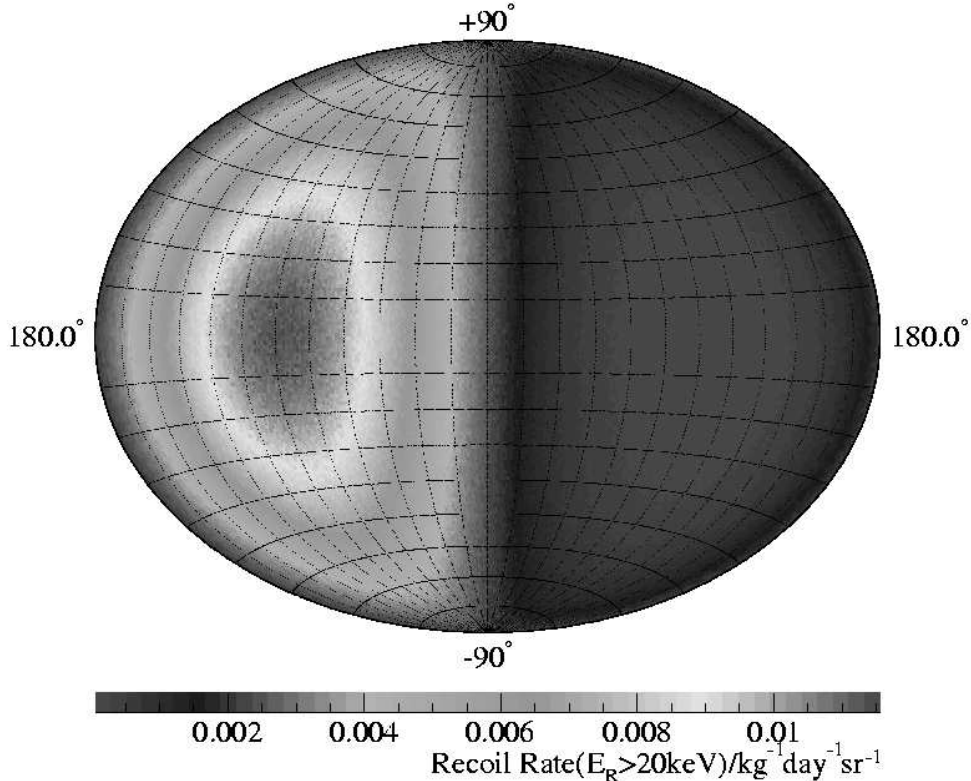


Fig. 1. The time averaged S recoil flux above 20 keV in Galactic (l,b) co-ordinates for the standard halo model, if the senses of the recoils can be measured and the uncertainty in the reconstruction of the recoil directions are included. The WIMP mass and cross-section are taken to be $m_\chi = 100$ GeV and $\sigma = 10^{-6}$ pb respectively and the local WIMP density is $\rho_0 = 0.3$ GeV cm $^{-3}$.

tion of the sidereal time dependent coordinate transformation to the detector frame, together with the 2-d projection effects described above. Further details of these procedures may be found in Refs [13,14]. The raw and reduced 2-d angle distributions are plotted in Fig. 2.

3 Statistical Tests of Isotropy in 2-d and 3-d

Recoil directions in 3-d and 2-d constitute points on the unit sphere and circle respectively. As we showed in Refs [13,14], experiments observing an anomalous recoil signal can confirm its Galactic nature by applying a range of simple non-parametric tests for anisotropy to the distribution of the observed recoil directions.

For 3-d data the most powerful test for rejecting isotropy uses the fact that, for smooth halo models, the WIMP recoil distribution is expected to be peaked about the direction of solar motion (l_\odot, b_\odot). It involves calculating the average

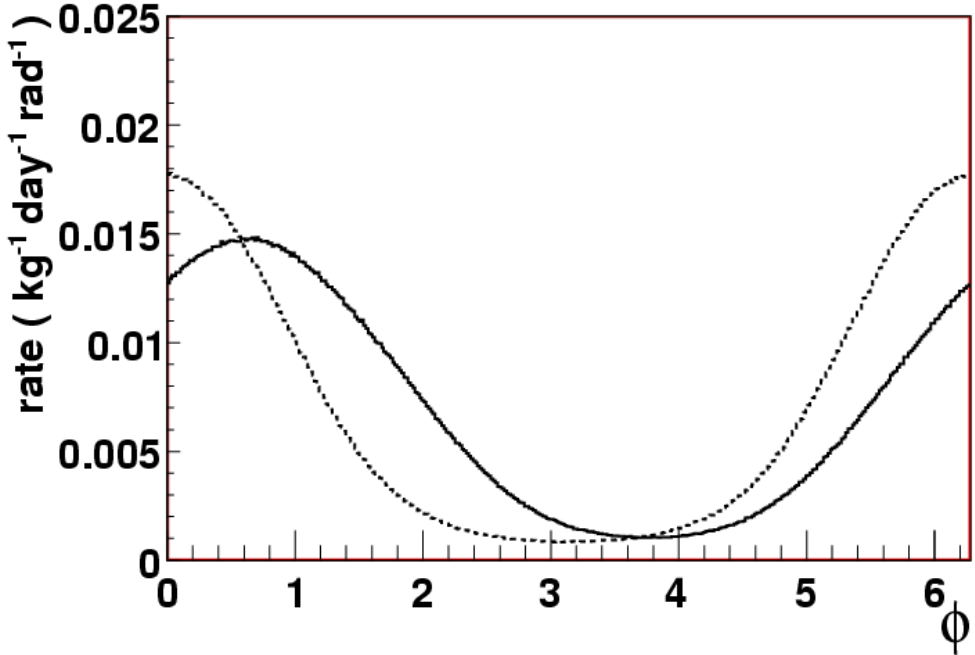


Fig. 2. The 2-d raw (solid line) and reduced (dotted line) angle distributions in the optimal read-out plane. The WIMP parameters are the same as for the 3-d recoil flux distribution in Fig. 1, from which the 2-d angle distributions are generated.

of the cosine of the angle between the direction of solar motion and the recoil direction. For the case when the sense of the recoil vectors are known

$$\langle \cos \theta \rangle = \frac{\sum_{i=1}^N \cos \theta_i}{N}, \quad (3)$$

where N is the number of vectors (i.e. the number of events), and if the recoil sense is not known then

$$\langle |\cos \theta| \rangle = \frac{\sum_{i=1}^N |\cos \theta_i|}{N}, \quad (4)$$

where θ_i is the 3-d angle between (l_\odot, b_\odot) and the i th vector/axis. For isotropic vectors $\langle \cos \theta \rangle$ ($\langle |\cos \theta| \rangle$) can take values on the interval $[-1, 1]$ ($[0, 1]$) and, due to the central limit theorem, approaches a gaussian distribution with mean 0 (0.5) and variance $1/3N$ ($1/3N$) [20] for large N . The larger the concentration of recoil directions towards (l_\odot, b_\odot) the larger these statistics will be. The probability distribution function of $\langle \cos \theta \rangle$ and $\langle |\cos \theta| \rangle$ as a function of N for the null hypothesis of an isotropic recoil spectrum has to be calculated by Monte Carlo simulation for small values of N .

For 2-d data we found in Ref. [14] that the most powerful test is the Rayleigh test which uses the mean resultant length of the projected recoil vectors which, modulo fluctuations, should be zero for data drawn from an isotropic distribu-

tion. For 2-d vectors, parameterized in terms of the angle ϕ (relative to some arbitrary fiducial direction), if we define

$$C = \sum_{i=1}^N \cos \phi_i, \quad (5)$$

$$S = \sum_{i=1}^N \sin \phi_i, \quad (6)$$

then the resultant length of the sum of the vectors, \mathcal{R} , is given by $\mathcal{R}^2 = C^2 + S^2$ and the mean resultant direction is $\bar{\mathcal{R}} = \mathcal{R}/N$. The modified Rayleigh [21] statistic \mathcal{R}^* , defined as [22,23]

$$\mathcal{R}^* = \left(1 - \frac{1}{2N}\right) 2N\bar{\mathcal{R}}^2 + \frac{N\bar{\mathcal{R}}^4}{2}. \quad (7)$$

has the advantage of approaching its large N asymptotic distribution for smaller values of N than $\bar{\mathcal{R}}$. Under the null hypothesis that the distribution from which the sample of angles is drawn is isotropic, \mathcal{R}^* is asymptotically distributed as χ_2^2 with error of order N^{-1} [23]. With axial data (i.e. unsigned lines) the standard procedure [24,25] is to double the axial angles, reduce them modulo 360° and analyze the resulting vector data.

For each detector configuration we calculate the probability distribution of the relevant statistic, for a given number of events N , by Monte Carlo generating 10^5 experiments each observing N recoils drawn from our simulated 3-d or 2-d distributions. We then compare this with the null distribution of the statistic, under the assumption of isotropy calculated using the analytic expression for the 2-d Rayleigh test and by Monte Carlo simulation for the 3-d $\cos \theta$ test. Specifically we calculate the rejection and acceptance factors, R and A , at each value T of the statistic. The rejection factor is the probability of measuring a value of the statistic less than T if the null (isotropic) hypothesis is true or equivalently the confidence with which the null hypothesis can be rejected given that measured value of the statistic. The acceptance is the probability of measuring a value of the statistic larger than T if the alternative hypothesis is true or equivalently the fraction of experiments in which the alternative hypothesis is true that measure a larger absolute value of the test statistic and hence reject the null hypothesis at confidence level R . Clearly a high value of R is required to reject the null hypothesis. A high A is also required, otherwise any one experiment might not be able to reject the null hypothesis at the given R or the null hypothesis might be erroneously rejected. We therefore find, using a search by bi-section, the number of events required for $A_c = R_c = 0.9$ and 0.95. For further details on this procedure see Appendix C of Ref. [13].

difference from baseline configuration	N_{90}	N_{95}
none	7	11
$E_T = 0$ keV	13	21
no recoil reconstruction uncertainty	5	9
$E_T = 50$ keV	5	7
$E_T = 100$ keV	3	5
$S/N = 10$	8	14
$S/N = 1$	17	27
$S/N = 0.1$	99	170
3-d axial read-out	81	130
2-d vector read-out in optimal plane, raw angles	18	26
2-d axial read-out in optimal plane, raw angles	1100	1600
2-d vector read-out in optimal plane, reduced angles	12	18
2-d axial read-out in optimal plane, reduced angles	190	270

Table 1

The dependence of the number of events required to reject isotropy for $A_c = R_c = 0.9$ and 0.95 , N_{90} and N_{95} , on the detector configuration. The baseline configuration has 3-d vector read-out, energy threshold $E_{TH} = 20$ keV, no background ($S/N = \infty$) and the uncertainty in reconstructing the recoil directions taken into account. The second and third lines are (unrealistic) improved configurations. The subsequent lines are degraded configurations. For the non-zero background configurations the numbers given are the number of *signal* events required.

4 Results

As our baseline optimistic, but realistic, detector configuration we consider a detector with 3-d vector (i.e. with recoil sense measurable) read-out, energy threshold $E_{TH} = 20$ keV, no background ($S/N = \infty$) and with the uncertainty in reconstructing the recoil directions taken into account. One or two of these specifications are varied in each of the alternative configurations. We consider two improved (and unrealistic) configurations, one with $E_{TH} = 0$ keV and one with perfect recoil reconstruction (since the recoil reconstruction can not be taken into account for 2-d read-out, the number of events required for 2-d read-out should be compared with this later 3-d configuration). We also consider a number of ‘degraded’ configurations: 2-d read-out, axial read-out, a larger energy threshold and non-zero background. For the 2-d read-out we consider both the raw angles and the reduced angles (with the projected direction of solar motion subtracted). We parameterize non-zero background in two different ways: variable signal to noise and variable background rate.

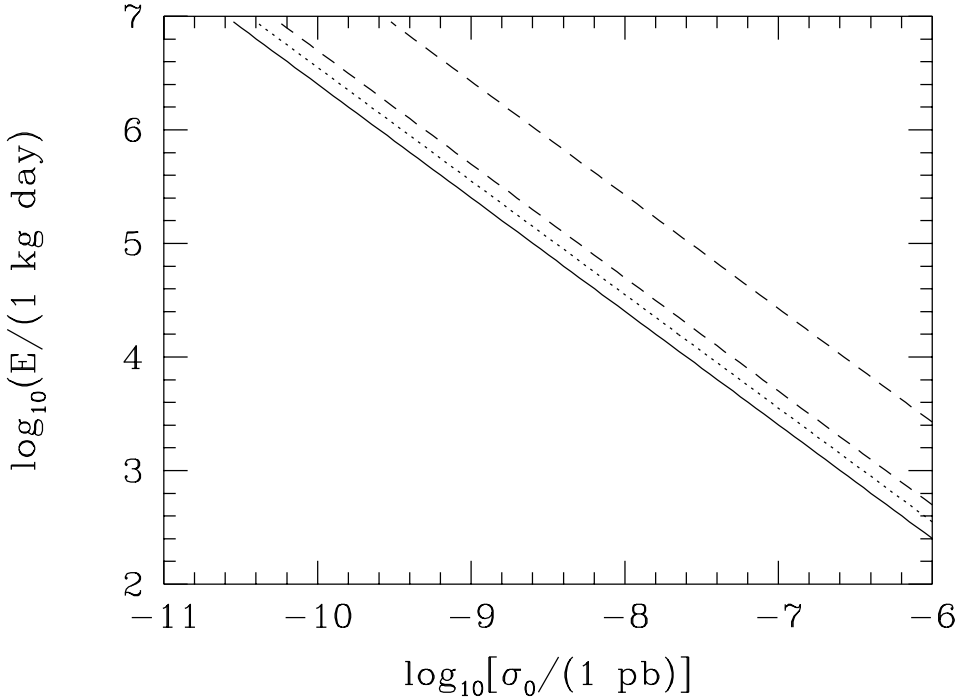


Fig. 3. The exposure required to reject isotropy (and detect a WIMP signal) at 95% confidence in 95% of experiments as a function of the WIMP-proton elastic scattering cross-section σ_0 , assuming a local WIMP density of $\rho = 0.3 \text{ GeV cm}^{-3}$. The solid line is for the benchmark configuration (zero background, $E_{\text{TH}} = 20 \text{ keV}$, 3-d vector read out). The dotted lines is $E_{\text{TH}} = 0 \text{ keV}$ and the dashed lines are, from bottom to top, 50 and 100 keV.

Table 1 gives the details of the configurations considered and the number of events required to reject isotropy (and hence detect a WIMP signal) at 90% (95%) confidence in 90% (95%) of experiments. The variable background rate configurations are not included in this table as in this case the number of events depends on the signal rate, and hence the cross-section. For the non-zero background cases we use a slightly different procedure to that described above, since the background and signal are both Poisson processes. In these cases for each value of the cross-section, we search for the required exposure by using the exposure, cross-section and signal to noise ratio (or background rate) to calculate the mean number of signal and background events. We then draw the number of signal and isotropic background events for each of the 10^5 experiments from Poisson distributions and calculate both the null and alternative distributions of the test statistic by Monte Carlo simulation. This procedure is not rigorously justified from a statistical point of view, but should not introduce significant bias/error.

In Figs. 3-7 we plot the exposure required to accumulate the required number of events for a 95% confidence detection in 95% of experiments as a function of the WIMP-nucleon elastic scattering cross-section σ_0 using the relationship

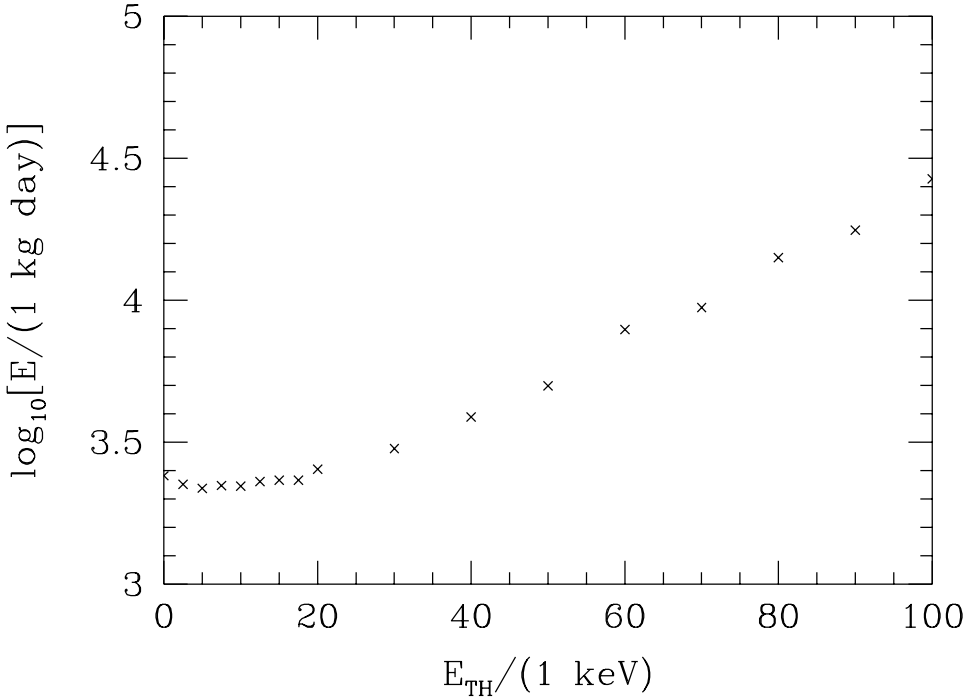


Fig. 4. The exposure required to reject isotropy (and detect a WIMP signal) at 95% confidence in 95% of experiments as a function of energy threshold, for WIMP-proton elastic scattering cross-section $\sigma_0 = 10^{-7}$ pb, assuming a local WIMP density of $\rho = 0.3$ GeV cm $^{-3}$.

$$E = \frac{N}{\sigma_0 R(> E_{\text{TH}})}, \quad (8)$$

where $R(> E_{\text{TH}})$ is the total event rate above threshold energy, per unit cross-section, assuming a fiducial local WIMP density $\rho_0 = 0.3$ GeV cm $^{-3}$ (the required exposure is inversely proportional to the local density). For the benchmark value $E_{\text{TH}} = 20$ keV, $R(> E_{\text{TH}}) = 1.5 \times 10^5$ kg $^{-1}$ day $^{-1}$ pb $^{-1}$, while for $E_{\text{TH}} = 0, 50$ and 100 keV, $R(> E_{\text{TH}}) = 2.9 \times 10^5, 4.7 \times 10^4$ and 6.2×10^3 kg $^{-1}$ day $^{-1}$ pb $^{-1}$ respectively ³. In each figure the solid line is the benchmark configuration (zero background, $E_{\text{TH}} = 20$ keV, 3-d vector read out), dashed lines are degraded configurations and dotted lines (where relevant) are unrealistic, optimistic configurations.

Figs. 3 and 4 show the effects of varying the energy threshold on the exposure required to reject isotropy. Fig. 3 shows the variation of the exposure

³ The event rates, especially for large threshold energies, depend on the Galactic escape velocity which is not well known. This dependence is not particularly strong and does not effect the conclusions of this work significantly.

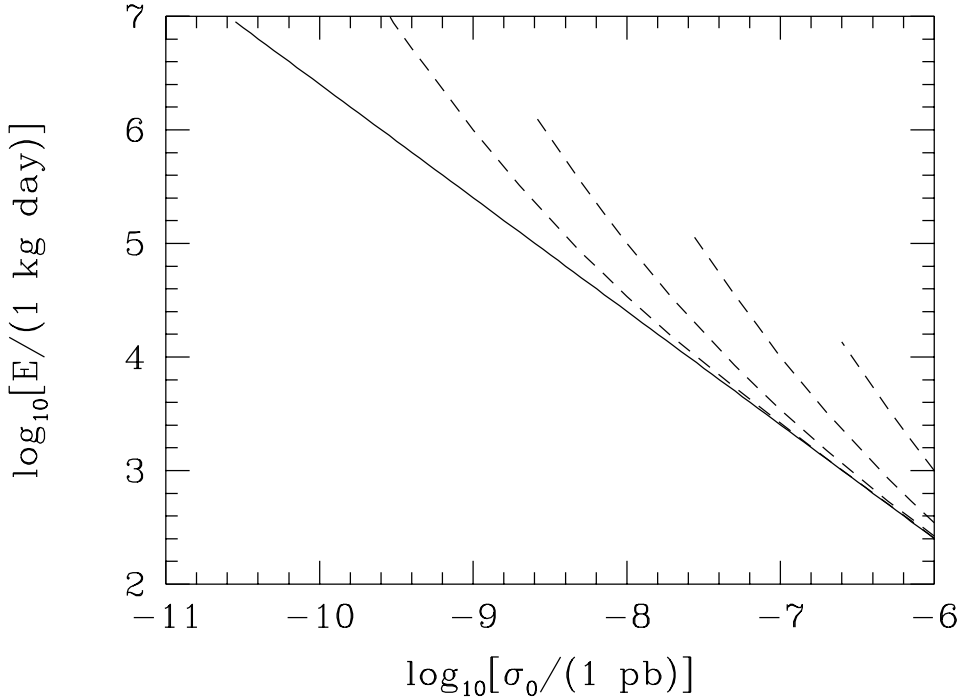


Fig. 5. As fig. 3. The solid line is for the benchmark configuration (zero background). The dashed lines are, (from right to left), background event rates of = 0.1, 0.01, 0.001 and $0.0001 \text{ kg}^{-1} \text{ day}^{-1}$.

with cross-section for four values of the energy threshold ($E_{\text{TH}} = 0, 20, 50$ and 100 keV) while Fig. 4 shows the variation with threshold energy for cross-section $\sigma_0 = 10^{-7} \text{ pb}$. As was pointed out by Spergel in the first paper on WIMP directional detection [3] there are two competing effects. The anisotropy of the recoils increases with increasing energy, so that the number of events required decreases, however the recoil rate also decreases. We find that the net effect is that the required exposure is fairly constant for $E_{\text{TH}} < 20 \text{ keV}$ and then increases with increasing threshold energy. The increase is not smooth, since the number of events required is an integer and has step-like variations at large threshold energies. As a rough indication, above 20 keV a 10 keV decrease in the energy threshold decreases the exposure required by roughly 25%. The quantitative variation of the exposure will depend on the detector composition, however we expect that this qualitative behaviour is fairly generic. Note that we have assumed in Fig. 4 that the recoil directions can be reconstructed down to $E = 0 \text{ keV}$. In reality it will be difficult, if not impossible, to reconstruct the direction of low energy recoils due to their short path-lengths.

Fig. 5 shows the variation of the exposure with cross-section for background rates of 0, 0.1, 0.01, 0.001 and $0.0001 \text{ kg}^{-1} \text{ day}^{-1}$. In each case the exposure curve follows the zero-background exposure curve at large cross-sections (where the signal rate is much larger than the background rate) before rising above the zero background curve, at first (when the signal and background rates are

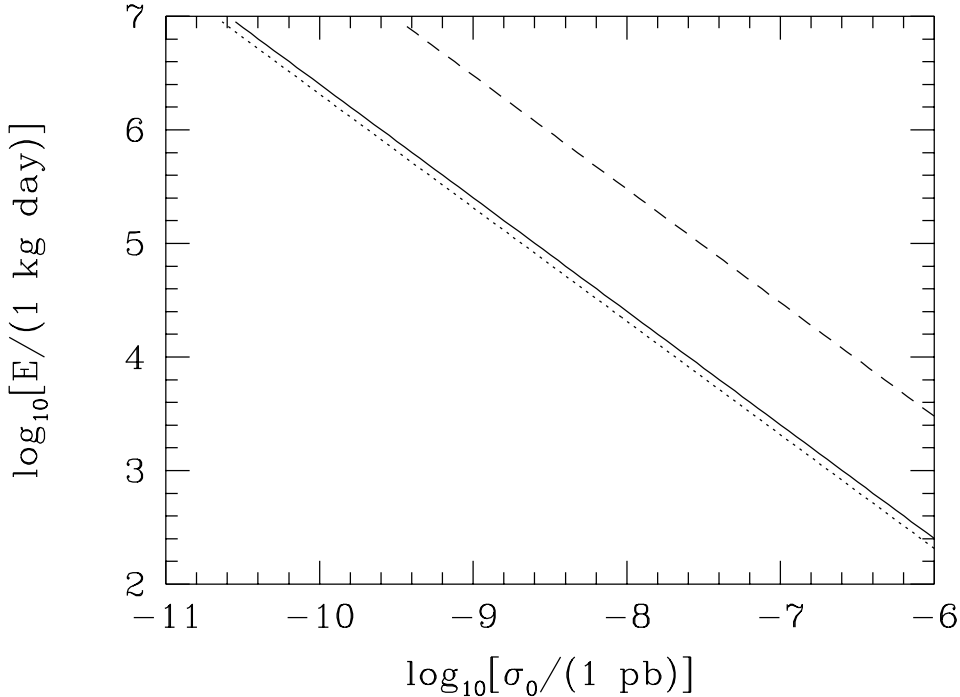


Fig. 6. As fig. 3. The solid line is for the benchmark configuration (3-d vector read out, recoil reconstruction uncertainty taken into account). The dotted line is 3-d vector read out ignoring the uncertainty in the reconstruction of the recoil direction. The dashed line is axial 3-d read-out.

comparable) gently and then (once the background rate is much greater than the signal rate) more rapidly. For fixed signal to noise ratio the number of events required is independent of cross-section and the corresponding exposure lines would lie parallel to the zero-background exposure line. When the background rate is the same as the signal rate the number of events, and hence the exposure, required is increased by a factor of ~ 2.5 . When the background is an order of magnitude bigger than the signal rate the increase is a factor of ~ 15 .

Fig. 6 shows the effects of the recoil reconstruction uncertainty and axial read-out in 3-d. The improvement which would come from perfect recoil reconstruction is relatively small, of order ten per-cent. If the read-out is axial rather than vectorial however, the exposure required is increased substantially, by more than an order of magnitude.

Fig. 7 compares 2-d read-out (vector and axial, and using raw and reduced angles) with 3-d read out. When the raw angles are used the exposure required is increased by a factor of ~ 3 for vectorial data, and by two orders of magnitude for axial data. Smaller exposures, in particular for axial data, can be achieved by using the reduced angles, which are measured relative to the (projected) direction of solar motion. Relative to 3-d vector read-out, the exposure using

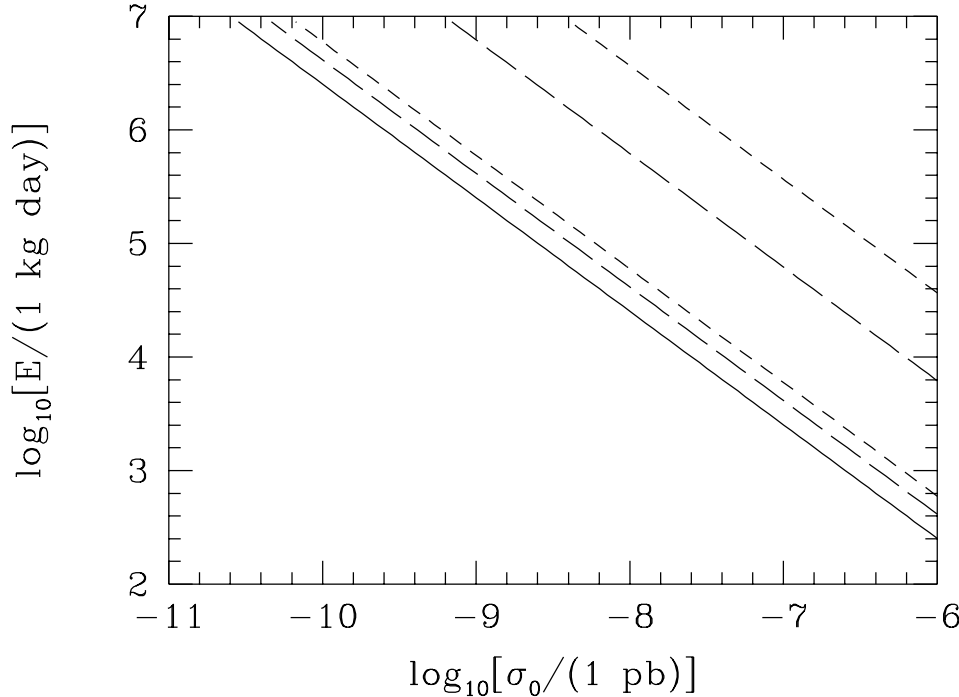


Fig. 7. As fig. 3. The solid line is for the benchmark configuration (3-d vector read-out, recoil reconstruction uncertainty taken into account). The short/long dashed lines are using raw/reduced angles for axial (top pair of lines) and vector (lower pair of lines) read-out.

reduced angles is increased by a factor $\sim 2/30$ for 2-d vector/axial read-out. These numbers are for read-out in the optimum plane, and are independent of the detector's geographical location. Read-out in other planes would lead to larger exposures by up to a factor of a few for vectorial raw and reduced angles and axial reduced angles and up to an order of magnitude for axial raw angles [14]. As the geographic location of the detector influences the orientation of these planes, the exposures for non-optimal planes vary by of order tens of per-cent between Boulby, Sudbury and Kamioka [14]. We should caution that the results for 2-d read-out assume a detector with perfect angular resolution. The projective effects of a 2-d read-out will make this a more significant factor than for 3-d read-out.

5 Conclusions

We have examined the effects of the detector properties on the number of events, and hence exposure, required to reject isotropy of recoil directions, and hence identify a putative WIMP signal as Galactic in origin. Specifically we have considered the nuclear recoil energy threshold, the background rate, 2-d and 3-d read-out and whether or not the sense of the recoils can be measured.

Our simulations are for a TPC detector filled with CS_2 . We expect that results for other directional detectors would be qualitatively similar.

We took a detector with 3-d vector read-out, energy threshold $E_{TH} = 20$ keV, no background ($S/N = \infty$), with the uncertainty in reconstructing the recoil directions taken into account, as our baseline realistic detector configuration and then varied one or two of these properties at a time. The property which has the largest effect on the exposure required is whether or not the sense of the recoils can be measured. If the data is axial (i.e. the sense can not be measured) the exposure is increased by one order of magnitude for 3-d read-out and two orders of magnitude for 2-d read-out compared to the baseline detector. With 2-d read-out this can be improved to a factor ~ 30 if the reduced angles (with the direction of solar motion subtracted) are calculated and analyzed. If the read-out is 2-d, and the senses can be measured, the exposure is increased by a factor of ~ 3 over the baseline. Once more this can be reduced, to a factor of ~ 2 , by using the reduced angles. These figures are for 2-d read-out in the optimal plane, which has normal perpendicular to the Earth's spin axis. For other read-out planes the required exposures are larger, and location dependent (see section 3 and Ref. [14] for further information). We also caution that the results for 2-d read-out assume perfect angular resolution, and projection effects will make this a more significant factor than for 3-d read-out. Estimates based on the projected length of recoil tracks in the planes indicate that the required exposure would increase by at least a factor 2 [14].

The effect of non-zero background depends on the underlying signal rate. If the signal and background rates are the same the exposure, relative to that for zero background, is increased by a factor of ~ 2.5 . If the background rate is an order of magnitude larger than the signal rate the increase is a factor of ~ 15 . As the signal to noise ratio is reduced below 0.1 the detection of the signal anisotropy becomes extremely challenging.

As the energy threshold is increased the WIMP recoil signal becomes increasingly anisotropic and the number of events required decreases. However the event rate decreases and the net effect is that the exposure required increases with increasing energy threshold above $E_{TH} \approx 20$ keV. The exposure increases by a factor ~ 1.3 for every 10 keV increase in the energy threshold. Below $E_{TH} \approx 20$ keV the exposure is roughly independent of the threshold energy. In practice achieving such low energy thresholds is not possible; the path lengths of low energy recoils are too short for the directions to be measured. We also caution that the actual 'energy threshold' of a directional detector is the maximum of the detection, discrimination and direction reconstruction thresholds.

In summary the property with the biggest effect on the detector performance

is whether or not the sense of the recoils can be measured. For 2-d read-out the performance, in particular if the senses can not be measured, can be significantly improved by recording and analyzing the reduced angles (with the projected direction of solar motion subtracted). The background rate effectively places a lower limit on the WIMP cross-section to which the detector is sensitive; it will be very difficult to detect a WIMP directional signal with a recoil rate more than an order of magnitude below the background rate. If the energy threshold is larger than about 20 keV significant improvements in the exposure required can be made by reducing the energy threshold (i.e. a factor of 2 if E_{th} is reduced from 50 keV to 20 keV and a factor of 5 if it is reduced from 100 keV to 50 keV).

References

- [1] M. W. Goodman and E. Witten, Phys. Rev. D 31, 3059 (1985).
- [2] A. K. Drukier, K. Freese and D. N. Spergel, Phys. Rev. D 33, 3495 (1986); K. Freese, J. Frieman and A. Gould, Phys. Rev. D 37, 3388 (1988).
- [3] D. N. Spergel, Phys. Rev. D 37, 1353 (1988).
- [4] G. Jungman, M. Kamionkowski and K. Griest, Phys. Rep. 267, 195 (1996).
- [5] J. D. Lewin and P. F. Smith, Astropart. Phys. 6, 87 (1996).
- [6] H. Kraus et al., Phys. Lett. B 610, 37 (2005).
- [7] D. P. Snowden-Ifft, C. J. Martoff, and J. M. Burwell, Phys. Rev. D 61, 1 (2000). Available from: astro-ph/9904064.
- [8] G. J. Alner et al., Nucl. Inst. and Meth. A. 535, 644 (2004).
- [9] T. Tanimori et al., Phys. Lett. B 578, 241 (2004). Available from: astro-ph/0310638.
- [10] C. J. Martoff, electronic proceedings of SNIC06 Symposium, California, 3-6 July 2006. Available from: <http://www-conf.slac.stanford.edu/snic/papers/0188.PDF>
- [11] C. J. Copi, J. Heo and L. M. Krauss, Phys. Lett. B 461, 43 (1999). Available from: astro-ph/990449; C. J. Copi and L. M. Krauss, Phys. Rev. D 63, 043507 (2001). Available from: astro-ph/0009467.
- [12] M. J. Lehner et al., *Dark Matter in Astro and Particle Physics*, Proceedings of the International Conference DARK2000, Heidelberg, Germany, 2000, p590 ed. H. V. Klapdor-Kleingrothaus, Springer-Verlag (2001).
- [13] B. Morgan, A. M. Green and N. J. C. Spooner, Phys. Rev. D 71 103507 (2005). Available from: astro-ph/0408047.

- [14] B. Morgan and A. M. Green, Phys. Rev. D 72, 123501 (2005). Available from: astro-ph/0508134.
- [15] C. J. Copi, L. M. Krauss, D. Simmons-Duffin and S. R. Stroiney, astro-ph/0508649.
- [16] D. Stiff and L. M. Widrow, Phys. Rev. Lett. 90, 211301 (2003). Available from: astro-ph/0301301.
- [17] B. Moore et al., Phys. Rev. D 64, 063508 (2002). Available from: astro-ph/010627.
- [18] J. F. Ziegler, J. P. Biersack and U. Littmark, *The stopping and range of ions in solids*, Pergamon Press (1985), <http://www.srim.org>.
- [19] M. J. Carson et al., Nucl. Inst. and Meth. A. 546, 509 (2005). Available from: hep-ex/0503017; M. J. Carson et al., Astropart. Phys. 21, 667 (2004).
- [20] M. S. Briggs, Astrophys. J. 407, 125, (1993).
- [21] Lord Rayleigh, Phil. Mag. 10, 73 (1880); Nature **72**, 318 (1905); Phil. Mag. 37, 321 (1918).
- [22] G. M. Cordeiro and S. Ferrari, Biometrika 78, 573 (1991).
- [23] K. V. Mardia and P. Jupp, *Directional Statistics*, Wiley, Chichester (2002).
- [24] W. C. Krumbein, J. Geology **47**, 673 (1939)
- [25] N. I. Fisher, *Statistical analysis of circular data*, CUP, (1993).
- .